JOURNAL OF APPLIED ELECTROCHEMISTRY 24 (1994) 767–771

Sparking at cathode tools during electrochemical machining in flow-through cells

I. ROUŠAR, T. RIEDEL

Department of Inorganic Technology, Institute of Chemical Technology, 166 28 Prague 6, Czech Republic

Received 26 January 1993; revised 9 June 1993

The current density used in electrochemical machining can be increased only up to a certain value, above which the formation of electric sparks on the cathode (tool) is observed, whereby the latter is damaged and the anode surface becomes rough. The present work is devoted to the measurement of this critical density for small metal cathodes placed on the wall of a flow-through channel for Reynolds numbers from 1265 up to 5902 and static pressures ranging from 0.1 up to 1.0 MPa. The results are correlated by criterion equations which gave values of critical (sparking) cathodic current density, j_s, with an average error of 7.1% for laminar flow and 4.1% for turbulent flow. The equations can be used for the calculation of the sparking current density for industrial flow-through cells for electrochemical machining.

List of symbols

C_{pE}	specific heat of electrolyte ($J\,kg^{-1}\,K^{-1}$)
d_E	equivalent diameter of the inter electrode gap (m)
h	height of the inter electrode gap (channel) (m)
I_s	limiting current for sparking (A)
J_s	limiting current density for sparking ($A\,m^{-2}$)
K_L, K_T	constants in Equations 1(a) and (b)
L_C	characteristic length of the cathode (disc cathode diam.) (m)
L_D	length of the channel downstream the cathode (m)
Nu	Nusselt number, Equation 2
Nu_L, Nu_T	see Equations 14–17
P	static pressure in the interelectrode gap at the cathode (Pa)
P_0	reference pressure (0.1 MPa)
Pr	Prandtl number, Equation 4
R, S, U	exponents, Equation 1(a) and (b)
Re	Reynolds number, Equation 3
T_B	boiling point of the electrolyte at the given static pressure (K)
T_0	temperature of the inlet electrolyte (K)
v_E	linear velocity of electrolyte flow through interelectrode gap (channel) ($m\,s^{-1}$)
w	width of the interelectrode gap (channel) (m)
$\Delta P_L, \Delta P_T$	pressure loss in the channel downstream the cathode (Pa)
ΔT	characteristic temperature difference (K)
$\Delta T_L, \Delta T_T$	see Equations 6, 7, 10 and 11 (K)

Greek symbols

κ_E	conductivity of electrolyte ($\Omega^{-1}m^{-1}$)
λ_E	heat conductivity of electrolyte ($W\,m^{-1}\,K^{-1}$)
μ_E	dynamic viscosity of electrolyte ($kg\,m^{-1}\,s^{-1}$)
ρ_E	electrolyte density ($kg\,m^{-3}$)

Subscripts

L	laminar flow (Re < 2300)
T	turbulent flow (Re > 2300)

1. Introduction

The principle of electrochemical machining [1] is the anodic dissolution of workpiece in a flowing electrolyte. The shape of the tool as cathode is copied into the workpiece as anode with relatively small deviations given by the width of the gap between the material and the tool. By increasing the rate of removal, not only can the process be accelerated but the machined surface becomes smoother [2]. However, the current density on the tool (cathode) can be increased only up to a certain limiting value given by the shape of the tool and hydrodynamic conditions. A further increase in current density causes the formation of electric sparks on the cathode [3–6], whereby the latter is damaged and the anode surface becomes rough.

Sparking during electrochemical machining was also studied by Drake and McGeough [7] who described an efficient method for drilling by simultaneous ECM and electrochemical arc machining (ECAM).

The conditions of spark formation at the cathode during ECM drilling of small holes and related equations for the convective heat transfer (for the sparking region) at various hydrodynamic conditions in the working gap, electrolyte properties, and cathode tool dimensions were proposed in our earlier work

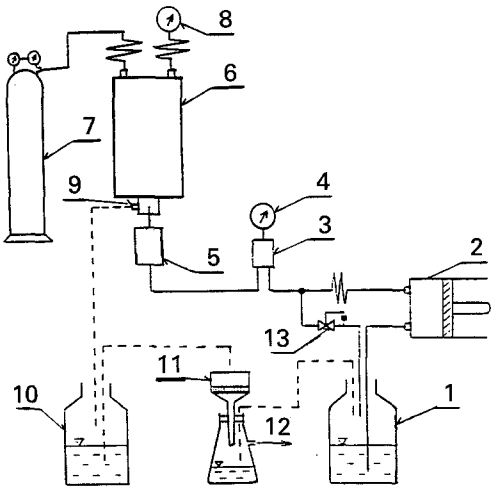

Fig. 1. Hydraulic diagram of the apparatus. (1) storage bottle, (2) piston pump, (3) air box, (4) manometer, (5) flow-through electrochemical cell, (6) pressurized vessel, (7) bottle with nitrogen (15 MPa), (8) manometer, (9) outlet valve, (10) reservoir, (11) filter glass fritted, (12) water pump, (13) safety valve.

[8] for a pressure of 0.1 MPa. The electrode processes at these conditions were also studied by Lazarenko and Lazarenko [9, 10] who found that the current passage through the electrolyte occurs in three distinct stages: (i) ionic conduction governed by Ohm's law, (ii) electric sparks, and (iii) electric arc.

The purpose of the present work was the measurement of the limiting current density at which the electric sparks are first observed in flow-through cells under elevated pressure.

2. Electric sparks in electrochemical machining

In a flow-through apparatus for electrochemical machining sparking always starts on such parts of the tool (cathode) which are nearest to the anode and where the local current density is much higher than the average current density. Such a situation can be simulated in a flow-through apparatus (Fig. 1) for electrochemical machining where the tool (cathode) is the tip of a metal wire of small active area (in our experiments we used 1 mm^2 active area in the form of a disc). An electrolyte flows through the channel into the gap between the workpiece and the tool.

When the terminal voltage of the electrolyser is gradually increased, the current flowing through it attains a critical (limiting) value. At this stage occasional electric sparks are observed on the surface of the cathode. On further increasing of the cell voltage, the current increases abruptly by 10–20% and begins to oscillate around a mean value which does not increase further. At the same time, acoustic and optical effects are observed: yellow–orange sparks or flames are visible at the cathode. Its metallic surface does not change in form, only blackens.

The following mechanism of sparking for a wire cathode was proposed in accordance with experiments reported in the literature [8, 11–13]; with respect to the distribution of current density at the cathode [14], the electrochemical process is concentrated on the tip of the wire cathode. The quantity of the evolved gas increases with current density. At the same time, a considerable amount of heat is evolved on the surface of the wire tip cathode. Heat is transferred to the electrolyte mainly by convection. Finally, the temperature of the electrolyte layer at the electrode attains the boiling point. Thus, together with the gas evolved electrolytically, a large number of bubbles appear at the electrode surface. The only paths for the passage, of current from the electrode surface to the bulk of electrolyte are the walls of the gas bubbles; the current density is correspondingly high, and the heating effect due to the Joule heat is very intense.

On increasing the voltage further, the electrolyte layer separating the bubbles begins to evaporate until it disappears to give a gas layer and the electric circuit is interrupted. A sufficiently high voltage causes ionization of the gas, leading to breakdown of the gas layer by electric discharge. The high temperature of the sparks causes evaporation of the metal and damage of both the cathode and workpiece.

3. Experimental details

3.1. *Measurements*

During electrochemical machining, it is necessary to prevent the current from surpassing the limiting value above which sparking begins, I_S. Since this depends on hydrodynamic conditions, composition of the electrolyte and on the static pressure in the gap between electrodes, we measured the dependence of I_S on the Reynolds number Re, and on the value of the ratio (P/P_0), where P_0 is the reference pressure, 0.1 MPa. The electrolyte velocity covered both the laminar and turbulent regions. Electrolyte data are given in Table 1; the electrolyte temperature at the inlet was 20 °C.

The measuring procedure was as follows. The rate of flow of the electrolyte through the channel and the pressure were adjusted. Then the electric current

Table 1. Characteristics of electrolytes used (20 °C) [16]

NaCl %	κ_E /$\Omega^{-1}\,m^{-1}$	ρ_E /$kg\,m^{-3}$	λ_E /$W\,m^{-1}\,K^{-1}$	$\mu_E \times 10^3$ /$kg\,m^{-1}\,s^{-1}$	c_{pE} /$J\,kg^{-1}\,K^{-1}$	*Pr*
2	3.4	1011	0.598	1.07	4250	7.605
5	6.7	1034	0.594	1.09	4050	7.432

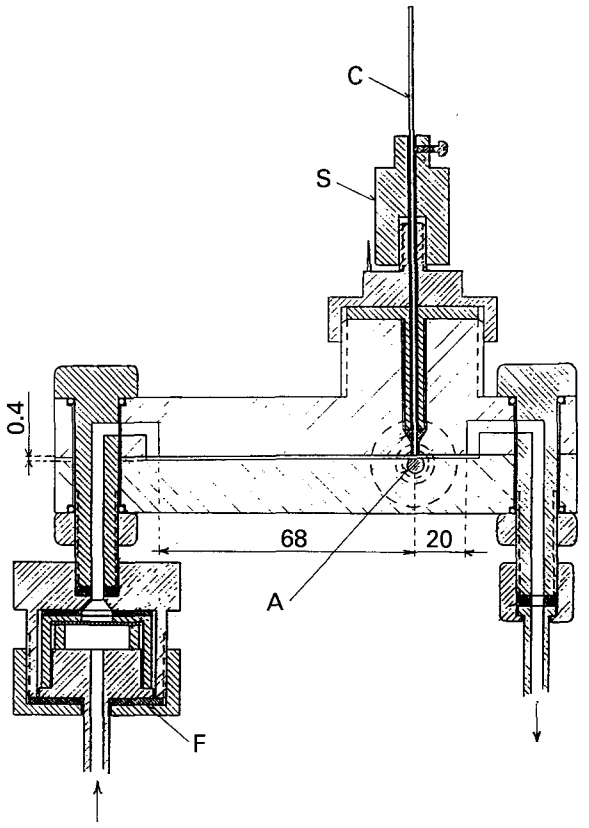

Fig. 2. Diagram of the electrochemical flow-through cell. (C) cathode, (A) anode, (S) micrometric screw, (F) high pressure filter.

was switched on and the voltage was gradually raised. The instant when sparks began to form at the cathode was determined visually in dimmed light and the corresponding value of I_S was measured. In total 24 data points were measured in the laminar flow region and 40 in turbulent flow (Figs 3, 4).

The current and voltage were measured with an accuracy of 1%. The accuracy of the average electrolyte flow rate was ±2%.

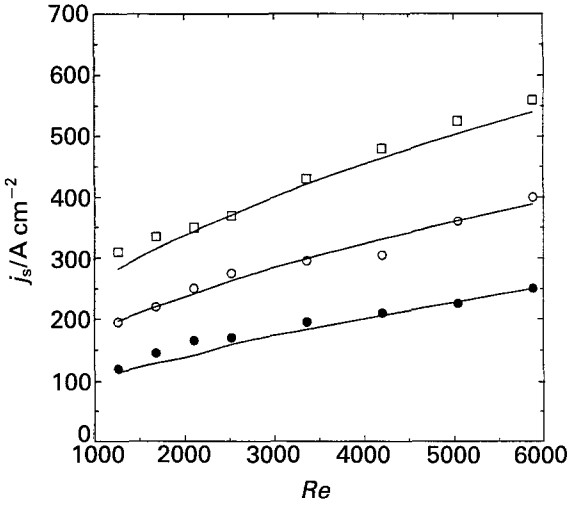

Fig. 3. The dependence of the sparking current density on Reynolds number for the electrolyte containing 2% NaCl for different static pressure P. Key: (●) 0.1 MPa, (○) 0.6 MPa and (□) 1.0 MPa. Experimental data are denoted by points, full lines were calculated using Equations 18 and 19.

3.2 *Apparatus*

The hydraulic circuit is shown in Fig. 1. Pure electrolyte flowed from a 25 dm^3 PVC storage bottle *1* by means of a piston pump *2* into the high-pressure compartment of the apparatus. It passed through a stainless pressure tubing into a high-pressure air box *3* to which a manometer *4* was connected. The air box smoothed out the pulses caused by the piston pump, enabling a constant rate of flow of the electrolyte to be maintained. The electrolyte passed further through an elastic copper spiral capillary into a flow-through electrochemical cell *5*. The electrolyte with the reaction products flowed from the electrochemical cell into stainless steel pressurized vessel *6*. This was filled with nitrogen from pressurized bottle *7* before the experiment at the desired pressure, measured by manometer *8*. The vessel *6* was provided with outlet valve *9* enabling the electrolyte to be discharged into reservoir *10* after the experiment.

Portions of the contaminated electrolyte with the slurry of $Fe(OH)_2$ from the pressurized vessel *6* were taken at intervals and filtered using a large fritted glass disc *11* (Kavalier, Czechoslovakia) connected to water pump *12*. The filtered solution was returned into the storage bottle *1*. The pressurized compartment of the apparatus was provided with safety valve *13* which was activated if the pressure exceeded about 10 MPa; in this case a portion of the electrolyte was allowed to pass into the storage bottle *1*.

In the present study the flow-through cell shown in Fig. 2 was used. Its body consisted of two rectangular blocks made of polymethylmethacrylate glass. One of the blocks carried a rectangular flow channel 0.4 mm deep, 4 mm wide and 88 mm long. A steel wire 1.13 mm in diameter (1 mm^2 cross-section area) was used as a fixed cathode and was positioned opposite the plate steel anode (3 mm × 4 mm active area). The plate anode was placed on the opposite side of the channel. The distance between the electrodes was 0.4 mm, i.e. the same as the channel depth, and was

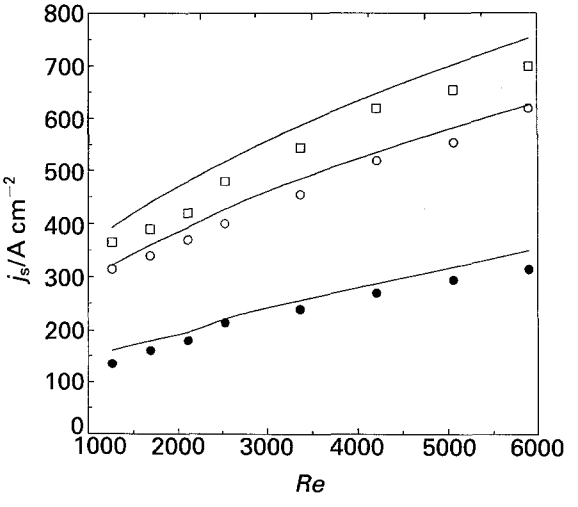

Fig. 4. The dependence of the sparking current density on Reynolds number for the electrolyte containing 5% NaCl for different static pressure P. Key as for Fig. 3.

adjusted by a micrometric screw. The leading edge of the working electrode was positioned 68 mm downstream from the flow channel inlet. The length of anode plate was 120 mm. After each measurement, which lasted approximately 10 s, the anode was advanced (4 mm) and a new anode surface appeared in the flow-through channel. This system of renewing the anode surface was necessary because the rate of dissolution of the anode was very high.

4. Results and discussion

In evaluating the measured data, it is assumed that the process of sparking is governed by heat transfer from the bubble-electrolyte layer formed at the cathode surface. The validity of the equations derived in earlier work [8] is assumed with a small modification due to the change of the static pressure in the inter-electrode space.

For the laminar regime,

$$Nu = K_L Pr^{0.4} Re^R (d_E/L_C)^S (P/P_0)^U \quad \text{for } Re < 2300 \tag{1a}$$

and for the turbulent regime

$$Nu = K_T Pr^{0.4} Re^R (P/P_0)^U \quad \text{for } Re > 2300 \tag{1b}$$

where

$$Nu = j_S^2 d_E^2/\kappa_E \lambda_E \Delta T \tag{2}$$

$$Re = v_E d_E \rho_E/\mu_E \tag{3}$$

$$Pr = c_{pE} \mu_E/\rho_E \tag{4}$$

$$d_E = 2wh/(w+h) \tag{5}$$

In all experiments d_E was 0.727 mm and L_C was 1.13 mm. Since the ratio d_E/L_C (0.727/1.13) was not varied the exponent S cannot be evaluated.

The evaluation of the unknown constants (R, U) in Equations 1(a) and (b) was done in two different ways:
(i) A new quantity ΔT^* was introduced, defined as

$$\Delta T_L^* = K_L \Delta T (d_E/L_C)^S \tag{6}$$

$$\Delta T_T^* = K_T \Delta T \tag{7}$$

Here, the value of ΔT is considered constant, independent of the boiling temperature at the given pressure and on the composition of the electrolyte. Thus,

$$\Delta T = T_S - T_0 \tag{8}$$

where T_S represents the cathode surface temperature during sparking. This characteristic temperature does not depend on other experimental conditions e.g. pressure, electrolyte composition etc.
(ii) The other possibility is to set the surface temperature T_S equal to the boiling temperature T_B,

$$\Delta T = T_B - T_0 \tag{9}$$

and to introduce the quantities

$$K_L^* = K_L (d_E/L_C)^S \tag{10}$$

$$K_T^* = K_T \tag{11}$$

After evaluation of the constants in Equations 1(a) and (b) on the basis of measured limiting current densities for sparking and different assumptions for ΔT, case (i) or (ii), a basic difference found is in the values of the exponent U (for pressure dependence). The boiling point T_B was evaluated for water [15] and a small correction due to the presence of 2% or 5% NaCl, viz 0.4 or 1.0 °C, was added [17].

The static pressure at the cathode was calculated from the measured static pressure in the reservoir *10*, Fig. 1 and the pressure loss in the channel downstream of the cathode was calculated from Equations 12 and 13 [18, 19].

$$\Delta P_L = (96/Re)(L_D/d_E) \tfrac{1}{2} \rho_E v_E^2 \quad \text{for } Re < 2300, \tag{12}$$

$$\Delta P_T = (0.3164/Re^{0.25})(L_D/d_E) \tfrac{1}{2} \rho_E v_E^2 \quad \text{for } Re > 2300 \tag{13}$$

where L_D represents the length of the channel downstream of the cathode (20 mm).

The measured data were correlated by Equations 1(a) and (b) rearranged by introducing ΔT^* or K^*, Equations 6, 7, 10 and 11, in the form, for case (i):

$$Nu_L^* = Pr^{0.4} Re^R (P/P_0)^U \tag{14}$$

$$Nu_T^* = Pr^{0.4} Re^R (P/P_0)^U \tag{15}$$

and for the case (ii):

$$Nu_L = K_L^* Pr^{0.4} Re^R (P/P_0)^U \tag{16}$$

$$Nu_T = K_T^* Pr^{0.4} Re^R (P/P_0)^U \tag{17}$$

For the case (i) we obtained

$$Nu_L^* = Pr^{0.4} Re^{0.78} (P/P_0)^{0.79} \quad \text{for } Re < 2300 \tag{18}$$

$$\Delta T_L^* = 566.5\,\text{K}$$

$$Nu_T^* = Pr^{0.4} Re^{0.86} (P/P_0)^{0.76} \quad \text{for } Re > 2300 \tag{19}$$

$$\Delta T_T^* = 326.5\,\text{K}$$

where

$$Nu^* = j_S^2 d_E L_C/\kappa_E \lambda_E \Delta T^* \tag{20}$$

For the case (ii) we obtained Equations 21 and 22

$$Nu_L = 7.04 Pr^{0.4} Re^{0.78} (P/P_0)^{0.48} \quad \text{for } Re < 2300 \tag{21}$$

$$Nu_T = 4.15 Pr^{0.4} Re^{0.85} (P/P_0)^{0.46} \quad \text{for } Re > 2300 \tag{22}$$

The exponents and characteristic temperature difference were determined from the data by the least squares method using modified Equations 14–17, e.g. their logarithmic form (see Appendix in [8]).

The average error of the critical current density, j_S, calculated using Equation 18 in the laminar region was estimated to be 7.1%. The average error of the critical current density, j_S, calculated using Equation

19 in the turbulent region was estimated to be 4.1%. Analogous values for Equations 21 and 22 were estimated to be 7.2% and 4.6%, respectively.

From the high exponent (0.47) for the pressure in Equations 21 and 22 it follows that the increase in boiling temperature with increase in pressure cannot explain (or fit) the pressure dependence of the sparking current densities. This means that the surface temperature T_S is much higher than the boiling temperature T_B. From the high exponent (0.78) for Reynolds number in Equations 18 or 21 it follows that the flow regime corresponds to transition from laminar to turbulent flow.

It may be concluded that Equations 18 and 19 can be recommended for the calculation of sparking current densities. These are local current densities on the projections of the cathode; for the laminar flow regime the projections should be approx. 1 mm in length (d_C) for interelectrode gap (h) 0.4 mm, or 0.5 mm in length for $h = 0.2$ mm. In the turbulent flow region there are no restrictions for the dimensions of the projections and for the dimensions of the interelectrode gap.

References

[1] J. F. Wilson, 'Practice and Theory of Electrochemical Machining', Wiley-Interscience, New York (1971) p. 11.

[2] H. Degenhardt, 'Elektrochemische Senkarbeit metallischer Werkstoffe', Thesis, Technische Hochschule Aachen, Aachen (1972) p. 92.

[3] R. A. Mirzoev, 'Cathode Process During ECM'. Collected papers on ECM, Schtiinca, Kischinev (1971) (in Russian).

[4] A. D. Davydov, V. D. Kaschtscheev and B. N. Kabanov, *Elektron. Obrab. Mater.* **6** (1969) 13.

[5] M. Datta and D. Landolt, *Electrochim. Acta* **26** (1981) 899.

[6] *Idem, ibid*, **27** (1982) 385.

[7] T. H. Drake and J. A. McGeough, Proceeding of Machine Tool Design and Research Conference, Macmillan (1981) p. 361.

[8] P. Novák, B. Sajdl, I. Roušar, *Electrochim. Acta* **30** (1985) 43.

[9] B. R. Lazarenko and N. I. Lazarenko, *Elektron. Obrab. Mater.* **1** (1978) 5.

[10] *Idem, ibid.* **1** (1966) 7.

[11] H. H. Kellogg, *J. Electrochem. Soc.* **48** (1950) 133.

[12] D. Landolt, R. Acosta, R. H. Muller, C. W. Tobias, *J. Electrochem. Soc.* **117** (1970) 839.

[13] I. M. Crichton, J. A. McGeough, E. Munro and C. White, 'Precision Engeering', July (1981) (cited in [7]).

[14] P. Novák, I. Roušar, A. Kimla, V. Mejta and V. Cezner, *Coll. Czech. Chem. Commun.* **46** (1981) 2949.

[15] V. Míka, L. Neužil, J. Vlček, Sbírka příkladů z chemického inženýrství, SNTL, Praha, 1981.

[16] R. A. Robinson, R. H. Stokes, 'Electrolyte Solutions', Butterworths, London (1961).

[17] International Critical Tables, Vol. III, 1st edition, McGraw-Hill, New York and London (1928) p. 326.

[18] M. Malinovský, I. Roušar a kol., 'Teoretické základy pochodů anorganické technologie I', SNTL, Praha (1987) p. 245.

[19] V. Míka, Základy chemického inženýrství, SNTL, Praha (1977) p. 144.